

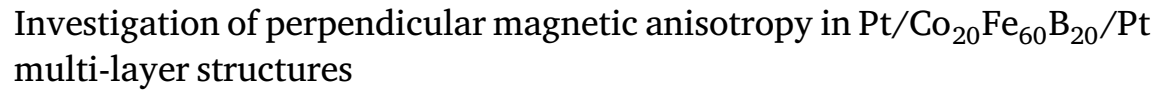
Contents lists available at ScienceDirect

Journal of Magnetism and Magnetic Materials

journal homepage: www.elsevier.com/locate/jmmm



Research article



Ludovico Cestarollo ^{a,*,1}, Karthik Srinivasan ^b, Amal El-Ghazaly ^b

- ^a Department of Materials Science and Engineering, Cornell University, Ithaca, NY 14853, United States of America
- b Department of Electrical and Computer Engineering, Cornell University, Ithaca, NY 14853, United States of America

ARTICLE INFO

Keywords: PMA Magnetic thin films CoFeB Pt Sputtering Magnetic properties

ABSTRACT

Multi-layers of $Co_{20}Fe_{60}B_{20}$ and Pt with large perpendicular magnetic anisotropies (PMA), comparable to those obtained with the more widely utilized Ta/CoFeB/MgO heterostructures, are reported. CoFeB thickness of approximately $0.8\,\mathrm{nm}$ is necessary to maximize PMA in Pt/CoFeB/Pt. Strong PMA can only be obtained upon careful tuning of the material the CoFeB layer is deposited on. Specifically, a Pt layer thickness of at least 3 nm is necessary to obtain PMA in CoFeB due to the emergence of (111) texture in thicker Pt films. The absence of a magnetic dead layer at the interface between CoFeB and Pt (as opposed to an interface between CoFeB and Ta) maximizes the amount of magnetic content per unit volume. Furthermore, this study investigates the magnetic properties of multi-layer structures where four CoFeB layers are deposited between Pt and Pt/Ta/Pt buffers. While the out-of-plane remanent magnetization of the structures is low, they present small nucleation field down to 30 Oe and large anisotropy energy in the range of $10^6\,\mathrm{erg/cc}$.

1. Introduction

The design and fabrication of thin-film heterostructures involving various combinations of metallic, oxide and ferromagnetic layers to achieve perpendicular magnetic anisotropy (PMA) has attracted a lot of interest in the field of spintronics. Specifically, magnetic tunnel junctions (MTJs) with PMA are of particular interest due to their high thermal stability and low current requirement for switching of the magnetization direction [1]. This magnetization switching is usually accomplished using spin-transfer torque (STT) or spin-orbit torque (SOT), depending on the materials in the heterostructure and the origin of spin polarization.

Multiple studies have focused on the development of heterostructures using pure Co as the ferromagnetic (FM) material. Co is often grown on textured Pt and capped with Pt (and/or Ta) non-magnetic metal (NM) layers to form single (one NM/FM/NM repetition) and multi-layer (multiple NM/FM/NM repetitions) stacks that have strong PMA [2–4]. Further reduction of the current needed to drive magnetization switching along with enhanced thermal stability at reduced dimensions and increased magnetoresistance ratio in tunnel junctions have made CoFeB the preferred ferromagnetic layer rather than pure Co [1,5]. However, the use of different CoFeB compositions reported in the literature makes a one-to-one comparison between these studies non-trivial [1,6–10]. Many of the reports involving CoFeB in the

20:60:20 (at.%) composition utilize Ta and MgO as respectively the bottom and top interfaces with the CoFeB layer [7,11–14]. However, in the absence of MgO, using Ta as either the seed and capping layer for the FM has proven to be detrimental to PMA [15,16]. Furthermore, Ta is known to intermix with CoFeB, creating a magnetic dead layer that lowers the overall magnetic fraction of the heterostructure [1, 11,17,18]. While not yet demonstrated, due to the Co content within CoFeB, we hypothesize that growing it on textured Pt can provide the interfacial properties needed to induce PMA in very thin films as it does with Co.

In this work we investigate the static magnetic properties of $\text{Co}_{20}\text{Fe}_{60}\text{B}_{20}$ single and multi-layer structures where the FM material (CoFeB in this case) is interfaced with Pt on both sides. The use of heavy metals presenting large spin Hall angle (such as Pt) is of interest when utilizing these structures for SOT applications. While, in theory, depositing the same heavy metal on both sides of the FM layer should cancel the spin–orbit torque efficiency, the differences in the interfacial characteristics between the top and bottom interfaces of the FM layer can result in an imbalance of torques, determining a net spin–orbit torque in the FM layer [3]. However, to the best of our knowledge, no study in the literature reports any consideration and/or result regarding $\text{Pt/Co}_{20}\text{Fe}_{60}\text{B}_{20}/\text{Pt}$ structures. Here we aim to address this gap and provide significant data regarding the PMA behavior of

E-mail addresses: lc942@cornell.edu (L. Cestarollo), ase63@cornell.edu (A. El-Ghazaly).

^{*} Corresponding author.

¹ This is the first author.

this specific system. Furthermore, we also report results about multi-layer $\text{Co}_{20}\text{Fe}_{60}\text{B}_{20}$ structures. This has not been done to date beyond investigating simpler bilayer stacks as done by Kaidatzis et al. [18] and Cheng et al. [19].

2. Materials and methods

The films were deposited in a high vacuum magnetron sputtering system (ATC Orion) from AJA International, Inc. under a base pressure of at least $10^{-7}\,\rm Torr$ on Si (100) substrates. All samples were sputtered at room temperature at a pressure of 3 mTorr while flowing Ar gas. No post-process annealing was performed. Heavy metals, being Ta and Pt, were sputtered using DC guns at powers of respectively 40 W and 20 W (which correspond to power densities of $1.97\,\rm W/cm^2$ and $0.99\,\rm W/cm^2$), yielding sputtering rates of 0.27 Å/s and 0.25 Å/s. The FM material, $\rm Co_{20}Fe_{60}B_{20}$ (denoted as CoFeB throughout the paper), was deposited using an RF gun at both 30 W and 100 W, yielding sputtering rates of 0.043 Å/s and 0.25 Å/s.

Magnetic measurements were performed via a vibrating sample magnetometry system (8600 Series VSM) from Lakeshore. All M vs. H hysteresis loops were recorded at room temperature. X-ray diffraction (XRD) was performed on the Ta/Pt structures using a Rigaku SmartLab X-ray diffractometer.

3. Results and discussion

3.1. Ta/Pt underlayers for PMA in CoFeB single-layer structures

The magnetic properties of the FM layer depend on the structure, crystallinity and thickness of the underlying Ta and Pt layers. Prior to the deposition of the FM layer, the structure of the Ta/Pt underlayer was investigated to determine the optimal thickness of Pt to be grown over the Ta seed layer. Reports from the literature indicate that Pt with (111) orientation is a suitable underlayer to obtain strong PMA in thin Co-containing (Co/Ni) films [15,20]. By starting with a 3 nm thick Ta seed (as similarly done in other studies [2,3]), Ta/Pt bilayer films with 2-5 nm of Pt were deposited and their structure was investigated using XRD. Fig. 1 shows the emerging of Pt (111) texture for Pt thicknesses of 3 nm or larger, indicating that Pt layers thinner than 3 nm do not posses the required polycrystallinity. Note that the Pt (111) peak is found at an angle of about 39.6°, in close agreement with the Pt powder diffraction pattern 243678 from the Inorganic Crystal Structure Database (ICSD) and other studies from the literature involving the growth of PMA stacks using Pt [15,20].

The impact of Pt structure on the magnetic properties of single-layer CoFeB systems was analyzed using M vs. H measurements of CoFeB films about $0.8\,\mathrm{nm}$ thick deposited on Ta $(3\,\mathrm{nm})/\mathrm{Pt}$ $(2\text{-}5\,\mathrm{nm})$. The structure was always capped with Pt $(5\,\mathrm{nm})$ to avoid the oxidation of the FM layer. While the stacks having 3-5 nm of Pt (as the underlayer) all show similar strong PMA behavior, the sample with the thinnest Pt underlayer $(2\,\mathrm{nm})$ shows a slanted out-of-plane (OOP) loop indicating a partial loss in PMA (refer to Figure S1 in the Supporting Information for these OOP and IP magnetization loops). The structure having $5\,\mathrm{nm}$ Pt underlayer provides a slightly higher remanence to saturation magnetization ratio, therefore this was selected as the optimal underlayer thickness to work with. These results highlight the importance of an appropriate Pt underlayer thickness (and therefore texture) to achieve strong PMA in $\mathrm{Co}_{20}\mathrm{Fe}_{60}\mathrm{B}_{20}$ -based structures.

3.2. Magnetic properties of CoFeB single-layer structures

A series of Ta (3 nm)/Pt (5 nm)/CoFeB (t)/Pt (5 nm) structures was prepared to study the effect of CoFeB thickness on anisotropy. The thickness of the CoBeB layer (sputtered at 100 W) was varied between 0.56 nm and 1.46 nm to capture both perpendicular magnetic anisotropy (PMA) and in-plane magnetic anisotropy (IMA) behaviors.

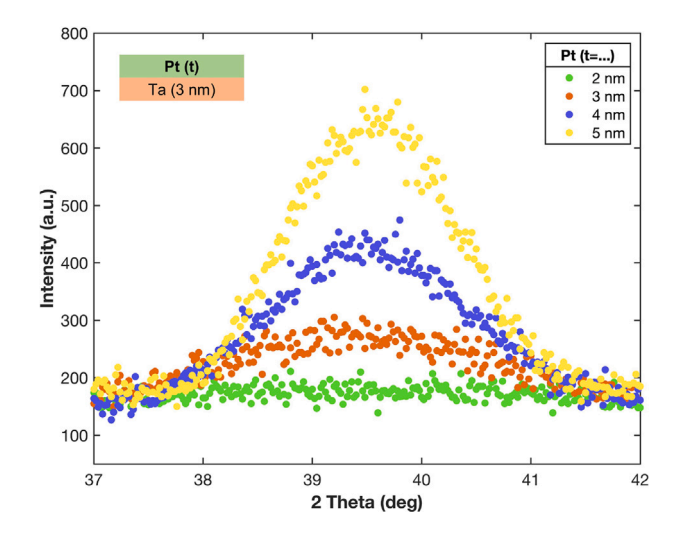


Fig. 1. XRD for 2 theta angles between 37° and 42° for the Ta $(3\,\text{nm})/\text{Pt}$ (t) structures with $t=2,\,3,\,4,\,5\,\text{nm}$.

Fig. 2a shows the saturation magnetization (Ms) measured for each structure as a function of the FM layer thickness. The average Ms was calculated to be 1230 emu/cc. This value agrees with the results from Ikeda et al. [1] and Cheng et al. [19], who report a saturation magnetization of 1260 emu/cc in the case of 1.3 nm thick CoFeB in a Ta/CoFeB/MgO heterostructure, and 1230 emu/cc for a double CoFeB layer in the MgO/CoFeB (0.8 nm)/Ta/CoFeB (1.2 nm)/MgO heterostructure, respectively. Our results show that the M_s values are within 8% of the calculated average for the different CoFeB thicknesses; Ms is not dependent on the thickness of CoFeB when bound by Pt on both the top and bottom surfaces. Furthermore, as illustrated in Fig. 2b, Ms.tCoFeB is linearly dependent on the thickness of the CoFeB layer and the fitting line possesses an x-axis intercept that is equal to $0.03 \, \mathrm{nm}$. The magnitude of this intercept indicates the thickness of the magnetic dead layer at the interfaces between CoFeB and the top and bottom Pt layers. Since this thickness is in the sub-angstrom range, it is concluded that the 0.03 nm is within the range of error and that the magnetic dead layer can be viewed as absent for the practical considerations of this study.

Given the prevalence in the literature of Ta as the underlayer of choice for CoFeB, Ta/CoFeB/Pt and Pt/CoFeB/Ta heterostructures were deposited to observe the effects of both Pt and Ta at either of the interfaces with the FM layer. In both cases PMA is lost and a significant reduction in saturation magnetization is recorded (refer to Figure S2 in the Supporting Information for more details). It is worth pointing out that no literature study explicitly states the impracticality of interfacing $\rm Co_{20}\rm Fe_{60}\rm B_{20}$ with both Pt and Ta. On the other hand, many studies report that Ta represents a good underlayer choice for a single CoFeB layer with the 20:60:20 composition when the top interface is MgO (or alternatively $\rm HfO_2$) [1,7,11–14,16,21–23]. At the same time, Ta is known to interdiffuse into CoFeB creating a magnetic dead layer of non-negligible thickness (even up to 0.7 nm), which in turn decreases the amount of magnetic content per unit volume, and, consequently, the saturation magnetization of the stack [1,11,17,18].

Furthermore, the anisotropy energy density ($K_{\rm eff}$) was calculated for each structure following the guidelines provided by Johnson et al. [24]. The thickness dependence of anisotropy energy densities for the deposited structures was analyzed by plotting $K_{\rm eff}$ - $t_{\rm CoFeB}$ as a function of $t_{\rm CoFeB}$, the thickness of the CoFeB layer (Fig. 2c). For larger thicknesses, the anisotropy energy is negative, indicating a preferential in-plane anisotropy with magnetic moments aligned in the plane of the film. As the thickness of CoFeB decreases, the anisotropy energy becomes less negative until it reaches a maximum positive value, before starting to

Table 1 Summary of K_{eff} and K_{eff} t_{CoFeB} values for some $Co_{20}Fe_{60}B_{20}$ -containing structures along with the results from our work.

Reference	Bottom interface	CoFeB	Top interface	$K_{eff} \cdot t_{CoFeB} \ (erg/cm^2)$	K _{eff} (erg/cc)
Kuswik et al. [5]	Au (10-60 nm)	0.9 nm	Au (2 nm)	7.50×10^{-5}	8.33×10^{2}
Kaidatzis et al. [18]	W (6 nm)	1.4 nm	MgO (2 nm)	0.250	1.79×10^{6}
Liu et al. [11]	Ta (5 nm)	1.1 nm	MgO (1 nm)/Ta (1 nm)	0.320	2.91×10^{6}
Ikeda et al. [1]	Ta (5 nm)	1.3 nm	MgO (1 nm)	0.273	2.10×10^{5}
This work	Pt (5 nm)	0.84 nm	Pt (5 nm)	0.085	1.01×10^{6}

decrease again for smaller thicknesses. This maximum $K_{\rm eff} \cdot t_{\rm CoFeB}$ value $(0.085\,{\rm erg/cm^2})$ occurs at an optimal FM layer thickness $(0.84\,{\rm m})$ where the heterostructure has the largest PMA energy density. The anisotropy energy densities from other literature reports on heterostructures with the same CoFeB composition are summarized in Table 1 along with the results from this study. While the anisotropy energy density of the Pt/CoFeB/Pt structure demonstrated here is three orders of magnitude larger than that of Au/CoFeB/Au [5], it is comparable to the energy densities of Ta/CoFeB/MgO heterostructures [1,5,11,18].

The volumetric and surface contributions to the anisotropy energy density are extrapolated from the plot in Fig. 2c. By performing a linear fit of the $K_{\rm eff}$ -t values for thicknesses between 0.84 nm and 1.46 nm, a slope of $-4.81 \times 10^6 \, {\rm erg/cc}$ and a y-axis intercept of 0.49 ${\rm erg/cm^2}$ are obtained. Given that $K_{eff} = K_v + K_s/t$ and $K_v = K_{bulk} - K_{shape}$, the slope of the line $K_{eff}t = K_vt + K_s$ corresponds to the difference between bulk and shape anisotropies, and the y-intercept is surface anisotropy. For the Pt/CoFeB/Pt system, surface anisotropy is comparable to that from literature works using Ta/MgO interfaces [1,18], while it is three orders of magnitude larger than that reported for the Au/CoFeB/Au heterostructure [5].

Fig. 3a and b illustrate respectively the OOP and IP magnetic hysteresis loops for the structures having CoFeB thicknesses of $0.56\,\mathrm{nm}$, $0.84\,\mathrm{nm}$ and $1.1\,\mathrm{nm}$. As mentioned above, the largest PMA energy density is observed at a FM layer thickness of $0.84\,\mathrm{nm}$ and this is reflected by an OOP loop with a high remanent to saturation magnetization ratio of 0.74. A weaker PMA (M_r/M_s ratio of 0.16) is observed with a thin CoFeB layer ($0.56\,\mathrm{nm}$), whereas thicker CoFeB ($1.1\,\mathrm{nm}$) presents IMA with the easy axis lying in the plane of the film.

Furthermore, PMA structures with CoFeB thickness around the optimal value were deposited by sputtering the FM layer at a lower power of 30 W. As shown in the K_{eff}·t_{CoFeB} vs. t_{CoFeB} plot from Fig. 2c, the anisotropy energies for these structures follow the trend for those with CoFeB sputtered at 100 W. Sputtering CoFeB at a lower power provides the advantage of more precise thickness control. In fact, by lowering the power from 100 W to 30 W, the sputtering rate is drastically reduced and therefore it is possible to sputter for longer times to consistently achieve the desired sub-nanometer thicknesses. Fig. 3c shows the hysteresis loops recorded in the case of 0.8 nm CoFeB sputtered at 30 W. For this film, strong PMA is still obtained, with a large remanent to saturation magnetization ratio of 0.76. As seen from the magnetic hysteresis loops in Fig. 3a and b (compared with those from Fig. 3c), there is no visible difference between the two films deposited with different CoFeB sputtering powers. All the multi-layer structures discussed in the next section utilize 30 W as the sputtering power for CoFeB.

3.3. Magnetic properties of CoFeB multi-layer structures

Once the thickness of a single CoFeB layer was optimized to maximize PMA, multi-layer CoFeB structures were prepared by depositing four 0.8 nm CoFeB layers separated by Pt buffers. In these multi-stack structures, the thicknesses of the Ta/Pt seed and the Pt cap were maintained equal to those utilized in the single FM layer study. As illustrated in Fig. 4a, first the thickness of the Pt buffer between each CoFeB layer in the stack was varied and M vs. H loops were recorded (here just the OOP loops are shown). While using a thin Pt layer of 1 nm does not result in PMA, PMA is observed for thicknesses larger than 3 nm. It is important to note that PMA is present in these

structures even if the remanent magnetization is comparably low. In fact, for all of these stacks the nucleation field (the magnetic field corresponding to which magnetization begins to switch as a result of domain nucleation) is smaller than 100 Oe, reaching a minimum of 40 Oe for thick Pt buffers of 8 nm. As multiple CoFeB layers are added to the stack, the roughness at the interfaces between CoFeB and Pt may increase, causing a reduction in surface anisotropy and therefore in remanent magnetization. Furthermore, the structural characteristics of the layers (roughness) are reported to influence the coupling between the ferromagnetic layers [25]. For the system under study, a thicker Pt buffer (>5 nm) is found to lower the nucleation field but at the same time it also reduces the magnetic fraction in the heterostructure, so a thinner Pt buffer that still guarantees good PMA is preferred (e.g. 3 nm).

In order to induce stronger PMA (and reduce the nucleation field), a structure with Pt buffers of 3 nm was grown while subjecting the substrate to an OOP field of about 140 mT during deposition. As expected, this resulted in a decrease in nucleation field from 90 Oe to 70 Oe due to an induced magnetic anisotropy. Further reduction to the nucleation field may be theoretically possible through smoother interfaces, which could be achieved by sputtering at higher powers to favor surface diffusion of Pt atoms impinging on the CoFeB. Therefore, a new heterostructure was fabricated by growing the Pt buffers at higher power (50 W, as opposed to the normally used 20 W). However, as seen in Fig. 4b, this latter attempt resulted in an increased nucleation field of 110 Oe. Sputtering Pt at higher power may have caused the roughness at the interfaces with CoFeB to increase, negatively affecting surface anisotropy [26,27].

Given that Ta was used as a seed layer to promote polycrystallinity in Pt (which is needed to obtain strong PMA in CoFeB films), multilayer CoFeB structures were deposited with Pt/Ta/Pt buffer layers (rather than just Pt). Note that Ta was not deposited in direct contact with the CoFeB layers because, as previously discussed, this would result in a magnetic dead layer due to interdiffusion. As illustrated in Fig. 4c, for these Pt/Ta/Pt buffers, the top Pt layer thickness was maintained at 3 nm, while the thicknesses of the bottom Pt and Ta layers were varied. It was found that these variations did not significantly change the magnetic behavior of the multi-stacks, but a non-negligible reduction in saturation magnetization was observed in the case of 1 nm Pt. Importantly, these results demonstrate that, by utilizing Ta as an underlayer for Pt within the buffers separating the CoFeB layers, the nucleation field can be further lowered to 30 Oe.

Fig. 5a illustrates the OOP and IP hysteresis loops for the multi-layer structure using Pt (3 nm)/Ta (3 nm)/Pt (3 nm) as the buffer. While high remanent magnetization is desired when designing devices that work at low fields (for example in the case of magnetic actuation [28]), large remanent magnetization is not a pre-condition for strong PMA. This structure presents the largest anisotropy energy (Keff) among all multilayer structures that were fabricated and characterized in this study. The calculated K_{eff} is $1.06 \times 10^6 \, erg/cc$, same as that for the optimal single-layer structure (see Table 1). The bow tie shape of the OOP hysteresis loop implies the presence of narrow magnetic domains with oppositely oriented moments (in the OOP direction) in each of the CoFeB layers. Due to the large thickness of the NM buffer layers, we eliminate the possibility of strong antiferromagnetic RKKY coupling between the magnetic layers and rather assume the behavior is due to a prevalence of ferromagnetic dipolar coupling between the CoFeB layers, a result similar to that illustrated by Maziewski et al. [29] for a

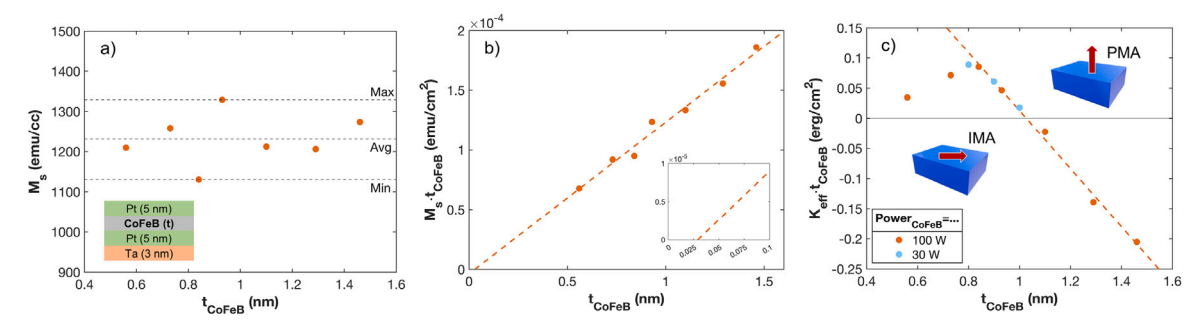


Fig. 2. Magnetic characterization of Ta (3 nm)/Pt (5 nm)/CoFeB (t)/Pt (5 nm) with CoFeB sputtered at 100 W: (a) Saturation magnetization vs FM layer thickness, where the upper and lower horizontal dashed lines correspond to the maximum and minimum values, which are within 8% of the average (center dashed line). (b) Estimation of magnetic dead layer from the linear fit (dashed line) of the M_s -t vs t data. Inset shows that the x-intercept is positive but very small, indicating the presence of an extremely thin (negligible for practical purposes) magnetic dead layer at the two CoFeB interfaces with Pt. (c) The K_{eff} -t vs t plot illustrates the variation in effective anisotropy energy with the FM layer thickness, identifying the optimal CoFeB thickness at around 0.8 nm. The data points for CoFeB sputtered at 30 W follow the same trend.

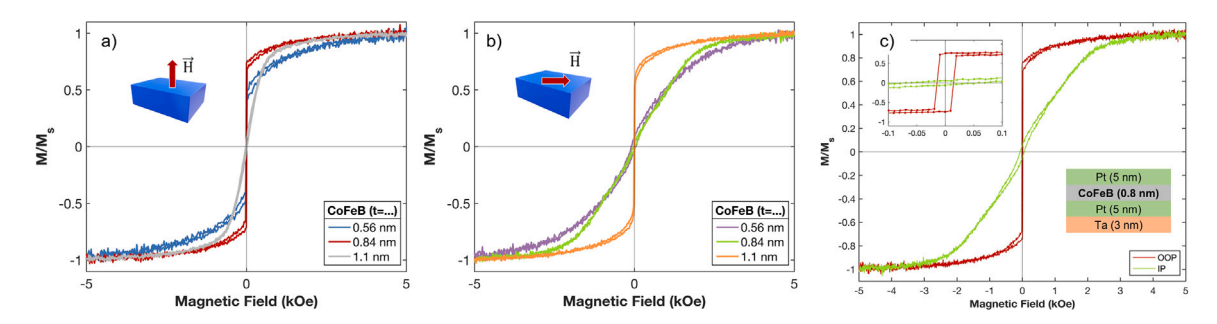


Fig. 3. The OOP and IP magnetic hysteresis loops for heterostructures with a single CoFeB layer (sputtered at 100 W) having thickness of 0.56, 0.84 and 1.1 nm are shown respectively in (a) and (b). The PMA energy density is maximum for 0.84 nm CoFeB, while for the 1.1 nm thick CoFeB the anisotropy has switched to in-plane (IMA). The OOP and IP loops for the structure with CoFeB sputtered at 30 W and optimal thickness (0.8 nm) are plotted together in (c), highlighting the presence of PMA.

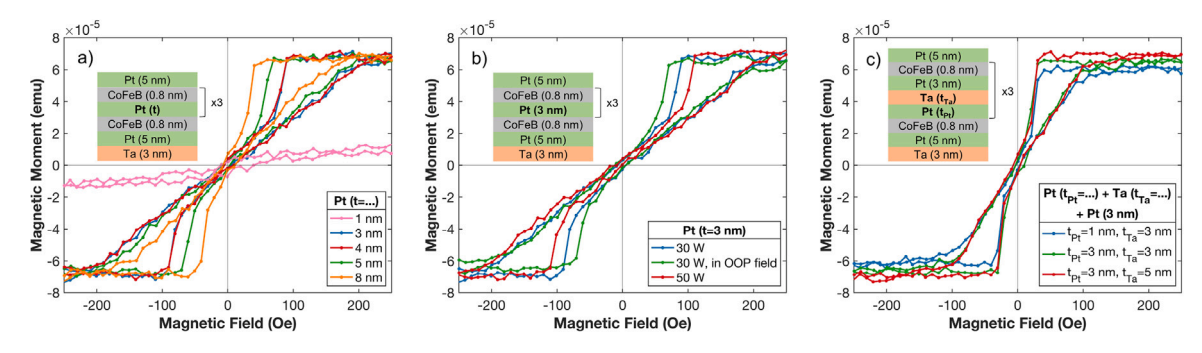


Fig. 4. Magnetic characterization of multi-layer heterostructures consisting of four CoFeB layers with: (a) Pt with varying thickness between CoFeB layers. Thicker Pt layers show a reduction in the OOP nucleation field. (b) 3 nm Pt between CoFeB layers deposited under different sputtering powers and in the presence of an OOP magnetic field. (c) Pt/Ta/Pt between each CoFeB layer. A low nucleation field of 30 Oe is obtained when multi-layers of CoFeB are deposited on Pt/Ta/Pt. A schematic illustration of the deposited heterostructures is shown in the insets of (a)–(c).

Co multi-layer structure. As shown in Fig. 5b, we hypothesize that the moments are pointing in the out-of-plane direction of the film. When the OOP magnetic field is applied, the domain walls move to expand the domains parallel to the field direction until the film saturates. In the IP case, the moments present no IP component in the remanent state thus yielding a remanent magnetization equal to zero, while as the magnetic field is applied, they slowly start to rotate and progressively align with the IP field direction saturating at a larger field of about 4kOe. Magnetic force microscopy image presented in Figure S3 in the Supporting Information verifies the nanoscale OOP domains in the remanent state of the multilayer CoFeB structure.

4. Conclusions

The relationship between texture in Pt grown with different thicknesses over Ta (3 nm) was investigated and it was found that Pt with

thickness of at least 3 nm is necessary to obtain polycrystalline Pt with (111) texture. The presence of Pt texture is correlated to the magnetic properties of the $\rm Co_{20}Fe_{60}B_{20}$ film deposited over it. When Pt (111) texture is present, the single-layer CoFeB structure shows strong PMA with large remanent to saturation magnetization ratio of up to 0.76. For the first time it was shown that depositing CoFeB (specifically with 20:60:20 at.% composition) between two layers of Pt can lead to strong PMA behavior, while growing CoFeB with Ta on the opposite interface leads to a total PMA loss (along with a drastic decrease in saturation magnetization). The optimal CoFeB thickness in single FM layer structures (Ta/Pt/CoFeB/Pt) was determined to be around 0.8 nm, with anisotropy energy ($\rm K_{eff}$) comparable to reports for Ta/CoFeB/MgO and orders of magnitude larger than for Au/CoFeB/Au.

Finally, multi-layer structures with four CoFeB layers separated by Pt buffers were deposited. The magnetic hysteresis loops show that thinner Pt buffers (1 nm) cause a total PMA loss, while thicker Pt yields

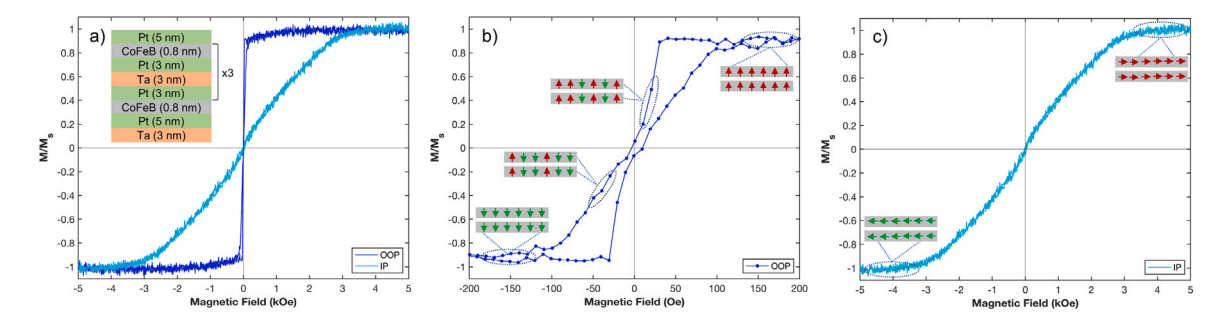


Fig. 5. M vs. H hysteresis loops for the Ta (3 nm)/Pt (5 nm)/CoFeB (0.8 nm)/[Pt (3 nm)/ToFeB (0.8 nm)]x3/Pt (5 nm) structure. Both OOP and IP loops are shown in (a). The moment orientations are illustrated in (b) and (c), for the OOP and IP loops respectively. While there are four ferromagnetic layers in the heterostructure, for simplicity the moment directions are illustrated only for two adjacent FM layers (in gray) separated by the buffer (in white). The other two moment directions would follow the same pattern.

good PMA and lower nucleation fields (adjacent CoFeB layers experience ferromagnetic dipolar coupling with parallel alignment in the OOP direction). By substituting the single material Pt buffers with trilayer buffers made of Pt/Ta/Pt it was possible to decrease the nucleation field down to 30 Oe. These results fill a gap currently present in the literature by showing that CoFeB with composition 20:60:20 can be interfaced solely with Pt to obtain strong PMA. This study encourages further exploration into material heterostructures that achieve PMA in CoFeB while utilizing different interface materials other than the more widely studied Ta and MgO.

CRediT authorship contribution statement

Ludovico Cestarollo: Conceptualization, Methodology, Validation, Formal analysis, Investigation, Writing – original draft, Writing – review & editing, Visualization, Project administration. **Karthik Srinivasan:** Conceptualization, Writing – review & editing. **Amal El-Ghazaly:** Resources, Writing – review & editing, Supervision, Funding acquisition.

Data availability

Data will be made available on request.

Acknowledgments

This work was primarily supported by and made use of the Cornell Center for Materials Research (CCMR) with funding from the NSF MRSEC program, United States of America (DMR-1719875). This work was performed in part at the Cornell NanoScale Facility, a member of the National Nanotechnology Coordinated Infrastructure (NNCI), which is supported by the National Science Foundation, United States of America (Grant NNCI-2025233).

Appendix A. Supplementary data

Supplementary material related to this article can be found online at https://doi.org/10.1016/j.jmmm.2022.169825.

References

- [1] S. Ikeda, K. Miura, H. Yamamoto, K. Mizunuma, H.D. Gan, M. Endo, S. Kanai, J. Hayakawa, F. Matsukura, H. Ohno, A perpendicular-anisotropy CoFeB-MgO magnetic tunnel junction, Nature Mater. 9 (2010) 721–724, http://dx.doi.org/ 10.1038/nmat2804.
- [2] S. Woo, M. Mann, A.J. Tan, L. Caretta, G.S. Beach, Enhanced spin-orbit torques in Pt/Co/Ta heterostructures, Appl. Phys. Lett. 105 (2014) http://dx.doi.org/10. 1063/1.4902529.
- [3] K.F. Huang, D.S. Wang, H.H. Lin, C.H. Lai, Engineering spin-orbit torque in Co/Pt multilayers with perpendicular magnetic anisotropy, Appl. Phys. Lett. 107 (2015) http://dx.doi.org/10.1063/1.4937443.

- [4] N.H. Kim, D.S. Han, J. Jung, K. Park, H.J. Swagten, J.S. Kim, C.Y. You, Dependence of interfacial Dzyaloshinskii-Moriya interaction and perpendicular magnetic anisotropy on the thickness of the heavy-metal layer, Appl. Phys. Express 10 (2017) http://dx.doi.org/10.7567/APEX.10.103003.
- [5] P. Kuswik, H. Glowinski, E. Coy, J. Dubowik, F. Stobiecki, Perpendicularly magnetized Co₂₀Fe₆₀B₂₀ layer sandwiched between Au with low Gilbert damping, J. Phys. Condens. Matter 29 (2017) http://dx.doi.org/10.1088/1361-648X/aa834d.
- [6] J.M. Iwata-Harms, G. Jan, S. Serrano-Guisan, L. Thomas, H. Liu, J. Zhu, Y.J. Lee, S. Le, R.Y. Tong, S. Patel, V. Sundar, D. Shen, Y. Yang, R. He, J. Haq, Z. Teng, V. Lam, P. Liu, Y.J. Wang, T. Zhong, H. Fukuzawa, P.K. Wang, Ultrathin perpendicular magnetic anisotropy CoFeB free layers for highly efficient, high speed writing in spin-transfer-torque magnetic random access memory, Sci. Rep. 9 (2019) http://dx.doi.org/10.1038/s41598-019-54466-7.
- [7] J. Kim, J. Sinha, M. Hayashi, M. Yamanouchi, S. Fukami, T. Suzuki, S. Mitani, H. Ohno, Layer thickness dependence of the current-induced effective field vector in Ta|CoFeB|MgO, Nature Mater. 12 (2013) 240–245, http://dx.doi.org/10.1038/nnat3522.
- [8] P. He, X. Qiu, V.L. Zhang, Y. Wu, M.H. Kuok, H. Yang, Continuous tuning of the magnitude and direction of spin-orbit torque using bilayer heavy metals, Adv. Electron. Mater. 2 (2016) http://dx.doi.org/10.1002/aelm.201600210.
- [9] R. Lavrijsen, Another spin in the wall: domain wall dynamics in perpendicularly magnetized devices, 2011, http://dx.doi.org/10.6100/IR693486.
- [10] A.S. Silva, S.P. Sá, S.A. Bunyaev, C. Garcia, I.J. Sola, G.N. Kakazei, H. Crespo, D. Navas, Dynamical behaviour of ultrathin [CoFeB (t_{CoFeB})/Pd] films with perpendicular magnetic anisotropy, Sci. Rep. 11 (2021) http://dx.doi.org/10.1038/s41598-020-79632-0.
- [11] Y. Liu, L. Hao, J. Cao, Effect of annealing conditions on the perpendicular magnetic anisotropy of Ta/CoFeB/MgO multilayers, AIP Adv. 6 (2016) http: //dx.doi.org/10.1063/1.4947132.
- [12] N. Vernier, J.-P. Adam, S. Eimer, G. Agnus, T. Devolder, T. Hauet, B. Ocker, F. Garcia, D. Ravelosona, Measurement of magnetization using domain compressibility in CoFeB films with perpendicular anisotropy, Sci. Adv. 104 (2014) http://dx.doi.org/10.1063/1.4869482\"\i.
- [13] J. Liu, T. Ohkulo, S. Mitani, K. Hono, M. Hayashi, Correlation between the spin Hall angle and the structural phases of early 5d transition metals, Appl. Phys. Lett. 107 (2015) http://dx.doi.org/10.1063/1.4937452.
- [14] G. Yu, Z. Wang, M. Abolfath-Beygi, C. He, X. Li, K.L. Wong, P. Nordeen, H. Wu, G.P. Carman, X. Han, I.A. Alhomoudi, P.K. Amiri, K.L. Wang, Straininduced modulation of perpendicular magnetic anisotropy in Ta/CoFeB/MgO structures investigated by ferromagnetic resonance, Appl. Phys. Lett. 106 (2015) http://dx.doi.org/10.1063/1.4907677.
- [15] E. Liu, J. Swerts, T. Devolder, S. Couet, S. Mertens, T. Lin, V. Spampinato, A. Franquet, T. Conard, S.V. Elshocht, A. Furnemont, J.D. Boeck, G. Kar, Seed layer impact on structural and magnetic properties of (Co/Ni) multilayers with perpendicular magnetic anisotropy, J. Appl. Phys. 121 (2017) http://dx.doi.org/ 10.1063/1.4974885.
- [16] T. Liu, J.W. Cai, L. Sun, Large enhanced perpendicular magnetic anisotropy in CoFeB/MgO system with the typical Ta buffer replaced by an Hf layer, AIP Adv. 2 (2012) http://dx.doi.org/10.1063/1.4748337.
- [17] S.Y. Jang, S.H. Lim, S.R. Lee, Magnetic dead layer in amorphous CoFeB layers with various top and bottom structures, J. Appl. Phys. 107 (2010) http://dx.doi. org/10.1063/1.3355992.
- [18] A. Kaidatzis, D.B. Gopman, C. Bran, J.M.G. a Martín, M. Vázquez, D. Niarchos, Investigation of split CoFeB/Ta/CoFeB/MgO stacks for magnetic memories applications, J. Magn. Magn. Mater. 473 (2019) 355–359, http://dx.doi.org/10.1016/ j.jmmm.2018.10.103.
- [19] H. Cheng, J. Chen, S. Peng, B. Zhang, Z. Wang, D. Zhu, K. Shi, S. Eimer, X. Wang, Z. Guo, Y. Xu, D. Xiong, K. Cao, W. Zhao, Giant perpendicular magnetic anisotropy in mo-based double-interface free layer structure for advanced magnetic tunnel junctions, Adv. Electron. Mater. 6 (2020) http://dx.doi.org/10.1002/aelm.202000271.

- [20] D. Rafaja, J. Vacínová, V. Valvodá, X-ray study of Co Ni and Co Pt Ni Pt multilayers, Thin Solid Films 374 (2000) 1020, http://dx.doi.org/10.1016/ S0040-6090(00)01072-5.
- [21] R. Pachat, D. Ourdani, J.W. van der Jagt, M. a Syskaki, A.D. Pietro, Y. Roussigné, S. Ono, M.S. Gabor, M. Chérif, G. Durin, J. Langer, M. Belmeguenai, D. Ravelosona, L.H. Diez, Multiple Magnetoionic Regimes in Ta/Co₂₀ Pe₆₀B₂₀/HfO₂, Phys. Rev. A 15 (2021) http://dx.doi.org/10.1103/PhysRevApplied.15.064055\"\"\i
- [22] P.J. Chen, Y.L. Iunin, S.F. Cheng, R.D. Shull, Underlayer effect on perpendicular magnetic anisotropy in $\text{Co}_{20}\text{Fe}_{60}\text{B}_{20}/\text{MgO}$ films, IEEE Trans. Magn. 52 (2016) http://dx.doi.org/10.1109/TMAG.2015.2511662.
- [23] F. Xue, N. Sato, C. Bi, J. Hu, J. He, S.X. Wang, Large voltage control of magnetic anisotropy in CoFeB/MgO/OX structures at room temperature, APL Mater. 7 (2019) http://dx.doi.org/10.1063/1.5101002.
- [24] M.T. Johnson, J.H. Bloemen, J.A.D. Broeder, J.J.D. Vries, Magnetic anisotropy in metallic multilayers, Rep. Progr. Phys. 59 (1996) 1409–1458, http://dx.doi. org/10.1088/0034-4885/59/11/002.
- [25] J. Moritz, F. Garcia, J.C. Toussaint, B. Dieny, J.P. Nozières, Orange peel coupling in multilayers with perpendicular magnetic anisotropy: Application to (Co/Pt)based exchange-biased spin-valves, Europhys. Lett. 65 (2004) 123–129, http: //dx.doi.org/10.1209/epl/i2003-10063-9.

- [26] Z. Xu, L. Qin, Effects of sputtering parameters and annealing temperatures on magnetic properties of CoFeB films, J. Magn. Magn. Mater. 538 (2021) http://dx.doi.org/10.1016/j.jmmm.2021.168302.
- [27] C. Zhou, T. Li, X. Wei, B. Yan, Effect of the sputtering power on the structure, morphology and magnetic properties of Fe films, Metals 10 (2020) 1–11, http://dx.doi.org/10.3390/met10070896.
- [28] L. Cestarollo, S. Smolenski, A. El-Ghazaly, Nanoparticle-based magnetorheological elastomers with enhanced mechanical deflection for haptic displays, ACS Appl. Mater. Interfaces 14 (2022) 19002–19011, http://dx.doi.org/10.1021/acsami.2c05471.
- [29] A. Maziewski, P. Kuswik, B. Szymański, F. Stobiecki, P. Mazalski, I. Sveklo, M. Tekielak, A. Kolendo, A. Maziewski, P. Kuświk, B. Szymański, F. Stobiecki, Magnetic properties of (Co/Au)N multilayers with various numbers of repetition N, Mater. Sci.-Poland 25 (2007).